Minimum Time Control of A Second-Order System

Zhaolong Shen and Sean B. Andersson
Department of Mechanical Engineering, Boston University, Boston, MA 02215
{zlshen,sanderss}@bu.edu

***Abstract*— A new algorithm for determining the switching time and final time for the minimum-time control of a second-order system is described. The system is driven from an initial state to a target state in minimum time. The controller is easy to design and implement, making it suitable for online implementation. Since the algorithm also produces the final time, it becomes feasible to optimize the switching sequence over a collection of states to be visited so as to minimize the total visiting time.**

I. Introduction

It is common to take measurements using a point or short-range sensor in many applications. For example, in scanning probe microscopy (SPM), the interaction between the probe and the sample surface is local. To image the sample, the generic approach is to raster scan the probe over the region of interest and rebuild the sample image pixel by pixel using the data collected on the regular grid. In recent years, non-raster scanning approaches have been proposed by researchers to reduce the imaging time by reducing the area to be sampled [1], [2]. Under such schemes, the next sampling point is not necessarily near the current position of the probe, motivating us to move the probe from rest to rest in minimum-time to improve scanning speed and measurement accuracy.

It is well known that by applying Pontryagin's maximum principle (PMP) [3] or Bellman's principle of optimality [4], it can be proved that the solution to the time-optimal control for a linear system with bounded control is always a bang-bang controller with a switching number no larger than the system order [3]. Though bang-bang control can transfer the system from an initial state to a target state in minimum time by simply switching the control between the minimum and maximum value, it is not practical in most applications because of its sensitivity to disturbance, parameters variation and unmodeled dynamics [5].

Motivated by the above limitations, researchers have been striving to increase the robustness of the controllers while maintaining approximate time optimal performance for over forty years. The proximate time optimal servomechanism (PTOS) was developed for second-order and third-order system [5], [6]. Extended PTOS (XPTOS) and adaptive PTOS (APTOS) were proposed to address flexible dynamics in the system [7]–[9]. Recently, the shaped time-optimal servomechanism (STOS) was developed to modify the bang-bang control signal before it was applied to the system to eliminate the residual vibration due to the flexible modes [10], [11]. A comparison of input shaping and time-optimal flexible-body control was presented in [12]. The robust and state-constrained time optimal control problem were also considered in [13], [14] and [15]. Other approaches have also been proposed by researchers to achieve proximate time-optimal output transition. The feedforward minimum-time control of non-minimum-phase linear scalar systems for set-point regulation was presented in [16] by using the stable input-output dynamic inversion technique. The linear quadratic minimum time (LQMT) output-transition problem was also solved in [17] with energy constrain and pre- and post-actuation. The near time optimal controller for nonlinear second order system was also presented in [18], [19].

The above controllers have been applied successfully in many applications, such as to disk drive systems [10], [14], [20]. However, they do not provide an estimate of the transition time from one state to another. In applications that include a collection of states to be visited by the controller, such information is useful. A primary motivating example is that of 3-D particle tracking in a confocal microscope [21]–[23]. In this application, a collection of measurements is needed to estimate the position of the particle and the overall tracking speed is limited in part by how fast the system can move through the sequence of positions. To improve scanning speed and measurement accuracy, one not only needs to achieve the minimum-time transition from one state to another, but also to optimize the visiting sequence over all states that need to be visited. This requires us to estimate the transition time online between any two states before they are actually visited. In this paper, we develop a new method to numerically calculate online the switching and final time between any two system states of a stable second-order system based on the bang-bang solution.

This paper is organized as follows. In Section II, the solution of the time-optimal problem is given. In Section III, it is shown that the solution of the switching and final time is equivalent to finding a crossing point of two spiral curves under an affine mapping. From this mapping, the switching and final time can be calculated quickly based on the geometry of the mapping. In Section IV, simulation and experimental results are shown to demonstrate this approach. A brief discussion and concluding remarks are made in Section V.

II. Problem Formation

A. System Model

Consider a stable second-order system transfer function

$$\frac{X_s(s)}{U(s)} = \frac{b_1 s + b_2}{s^2 + a_1 s + a_2}, \tag{1}$$

where $x_s \in \mathbb{R}$ is the system position and $u \in [u_{min}, u_{max}] \subset \mathbb{R}$ is the (bounded) input control signal. Define the system states as

$$x_1 = x_s, \tag{2a}$$
$$x_2 = x_1 + \beta_1 u. \tag{2b}$$

Then the canonical controllable state-space model is given by

$$\dot{X} = AX + Bu, \tag{3}$$

where

$$X = \begin{bmatrix} x_1 \\ x_2 \end{bmatrix}, \quad A = \begin{bmatrix} 0 & 1 \\ -a_2 & -a_1 \end{bmatrix}, \quad B = \begin{bmatrix} \beta_1 \\ \beta_2 \end{bmatrix}. \tag{4}$$

β_i is given implicitly by

$$\begin{bmatrix} 0 \\ b_1 \\ b_2 \end{bmatrix} = \begin{bmatrix} 1 & 0 & 0 \\ a_1 & 1 & 0 \\ a_2 & a_1 & 1 \end{bmatrix} \begin{bmatrix} \beta_0 \\ \beta_1 \\ \beta_2 \end{bmatrix}. \tag{5}$$

We assume that the eigenvalues of A are given by

$$\lambda_{1,2} = -\frac{a_1}{2} \pm i\omega \tag{6}$$

where ω can be calculated as

$$\omega = \sqrt{4a_2 - a_1^2} \tag{7}$$

and assume that $\omega \neq 0$. (We note that the case of two pure real eigenvalues is a simpler version of the scheme presented here.) With these assumptions, the eigenvectors of A are

$$P = \begin{bmatrix} 1 & 1 \\ \lambda_1 & \lambda_2 \end{bmatrix}. \tag{8}$$

Thus,

$$P^{-1}AP = \begin{bmatrix} \lambda_1 & 0 \\ 0 & \lambda_2 \end{bmatrix}. \tag{9}$$

B. Minimum Time Control

We consider the following problem

Problem 1: Given the state-space model (3) of system (1) and the initial system state X_0, design a control law to drive system (3) to the target state X_r in minimum time.

■

To solve this problem, we define a new system state $\hat{X}$ and rewrite system (3) and the initial state X_0 as

$$\hat{X} = X - X_r, \tag{10a}$$
$$\dot{\hat{X}} = A\hat{X} + Bu + AX_r, \tag{10b}$$
$$\hat{X}_0 = X_0 - X_r. \tag{10c}$$

Then Problem 1 can be stated equivalently as:

Problem 2: Given system (10), design a control law to drive the system from the initial state $\hat{X}_0$ to the origin in minimum time.

■

This problem can be solved by using the PMP [3]. Because we want to minimize the control time, define the cost function as

$$J = \int_0^{t_f} 1\, dt. \tag{11}$$

Now, we apply the PMP as follows. Define the Hamiltonian of (10) as

$$H = 1 + \lambda^T (A\hat{X} + Bu + AX_r), \tag{12}$$

where λ is the state of the adjoint system of (10). The combined system is then given by

$$\dot{\hat{X}} = \frac{\partial H}{\partial \lambda} = A\hat{X} + Bu + AX_r, \tag{13a}$$
$$\dot{\lambda} = -\frac{\partial H}{\partial \hat{X}} = -A^T\lambda, \tag{13b}$$
$$H(t_f) = 1 + \lambda(t_f)^T (A\hat{X}(t_f) + Bu(t_f) + AX_r) = 0. \tag{13c}$$

Since the target state is the origin, we have

$$\hat{X}(t_f) = 0, \tag{14}$$

yielding, from (13c),

$$1 + \lambda(t_f)^T (Bu(t_f) + AX_r) = 0. \tag{15}$$

A control signal giving the minimum time is found by minimizing the Hamiltonian in (12). This yields

$$u(t) = \begin{cases} u_{\min}, & if \quad \lambda^T B > 0, \\ u_{\max}, & if \quad \lambda^T B < 0, \end{cases} \tag{16}$$

with the value of u arbitrary when $\lambda^T B = 0$. This is the bang-bang control law for the linear system. In general, there is no analytic solution for the combined system in (13) due to the lack of sufficient boundary conditions on the adjoint system. So, the switching function $\lambda^T B$ in the bang-bang control law (16) cannot be solved analytically. Though one can numerically solve λ with the gradient methods provided in [3], [24], the difficulty in making a good and meaningful initial guess of the costate λ and the time-consuming nature make it not practical for online implementation. Moreover, it does not provide the switching and final time explicitly. Such information is critical to optimize the total visiting time when moving through a collection of states.

III. Switching Time and Final Time

To simplify the presentation, we make the following definitions, assumptions and denotions for the calculation of the switching and final time. Define:

$$\begin{aligned} t_s &: \text{switching time}, \\ t_f &: \text{final time}, \\ \Phi(t,\tau) &: \text{state transition matrix}. \end{aligned} \tag{17}$$

We assume that the control signal is at u_{max} at the beginning of the bang-bang control until switching time t_s and then the control signal switches to u_{min} until final time t_f. (The other cases follow in similar fashion.) Define variables v, z, m, n, $\hat{x}_{01}$ and $\hat{x}_{02}$ as following:

$$AX_r + Bu_{\max} = [v \quad z]^T, \tag{18a}$$
$$AX_r + Bu_{\min} = [m \quad n]^T, \tag{18b}$$
$$\hat{X}_0 = [\hat{x}_{01} \quad \hat{x}_{02}]^T. \tag{18c}$$

The system state at time t_s is given by

$$\hat{X}(t_s) = \Phi(t_s,0)\hat{X}_0 + \int_0^{t_s} \Phi(t_s,t) \begin{bmatrix} v \\ z \end{bmatrix} dt. \tag{19}$$

From time t_s to t_f, the system is driven by control signal u_{min} with initial state $\hat{X}(t_s)$. So, the system state at time t_f is given by

$$\begin{aligned} \hat{X}(t_f) &= \Phi(t_f - t_s, 0)\hat{X}(t_s) \\ &\quad + \int_0^{t_f - t_s} \Phi(t_f - t_s, t) \begin{bmatrix} m \\ n \end{bmatrix} dt, \end{aligned} \tag{20}$$

Substituting (14) into (20) and multiplying $\Phi(t_s, t_f - t_s)$ on both sides of (20), we have

$$\begin{aligned} &- \int_0^{t_f - t_s} \Phi(0,t) \begin{bmatrix} m \\ n \end{bmatrix} dt \\ &= \Phi(t_s,0)\hat{X}_0 + \int_0^{t_s} \Phi(t_s,t) \begin{bmatrix} v \\ z \end{bmatrix} dt. \end{aligned} \tag{21}$$

Now, consider the three terms in (21). From (9), it can be shown that

$$\Phi(t_s,0) = P \begin{bmatrix} e^{\lambda_1 t_s} & 0 \\ 0 & e^{\lambda_2 t_s} \end{bmatrix} P^{-1}, \tag{22}$$

$$\begin{aligned} &\int_0^{t_s} \Phi(t_s,t)dt \\ &= P \begin{bmatrix} \frac{1}{\lambda_1}(e^{\lambda_1 t_s} - 1) & 0 \\ 0 & \frac{1}{\lambda_2}(e^{\lambda_2 t_s} - 1) \end{bmatrix} P^{-1}, \end{aligned} \tag{23}$$

and

$$\begin{aligned} &- \int_0^{t_f - t_s} \Phi(0,t)dt \\ &= P \begin{bmatrix} \frac{1}{\lambda_1}(e^{\lambda_1 (t_s - t_f)} - 1) & 0 \\ 0 & \frac{1}{\lambda_2}(e^{\lambda_2 (t_s - t_f)} - 1) \end{bmatrix} P^{-1}. \end{aligned} \tag{24}$$

Define

$$\tau = t_f - t_s, \quad R(t) = e^{-\frac{a_1}{2}t}. \tag{25}$$

Substituting (6) and (8) into (22), (23) and (24) and carrying out some straightforward but tedious calculations yields

$$\Phi(t_s,0)\hat{X}_0 = \begin{bmatrix} \hat{x}_{01}\cos(\omega t_s) + \frac{a_1\hat{x}_{01} + 2\hat{x}_{02}}{2w}\sin(\omega t_s) \\ \hat{x}_{02}\cos(\omega t_s) - \frac{2a_2\hat{x}_{01} + a_1\hat{x}_{02}}{2w}\sin(\omega t_s) \end{bmatrix} R(t_s), \tag{26}$$

$$\begin{aligned} \int_0^{t_s} \Phi(t_s,t) \begin{bmatrix} v \\ z \end{bmatrix} dt &= \begin{bmatrix} \frac{a_1 v + z}{a_2} \\ -v \end{bmatrix} + \\ &\begin{bmatrix} -\frac{a_1 v + z}{a_2}\cos(\omega t_s) + \frac{v(4w^2 - a_1^2) - 2a_1 z}{4a_2 w}\sin(\omega t_s) \\ v\cos wt_s \quad + \quad \frac{a_1 v + 2z}{2w}\sin(\omega t_s) \end{bmatrix} R(t_s), \end{aligned} \tag{27}$$

$$\begin{aligned} - \int_0^{\tau} \Phi(0,t) \begin{bmatrix} m \\ n \end{bmatrix} dt &= \begin{bmatrix} \frac{a_1 m + n}{a_2} \\ -m \end{bmatrix} + \\ &\begin{bmatrix} -\frac{a_1 m + n}{a_2}\cos(\omega\tau) - \frac{m(4w^2 - a_1^2) - 2a_1 n}{4a_2 w}\sin(\omega\tau) \\ m\cos(\omega\tau) \quad - \quad \frac{a_1 m + 2n}{2w}\sin(\omega\tau) \end{bmatrix} R(-\tau). \end{aligned} \tag{28}$$

Now, substitute (26), (27) and (28) into (21) and define

$$X(t) = R(t)\cos(\omega t), \quad Y(t) = R(t)\sin(\omega t), \tag{29}$$

$$A_1 = \begin{bmatrix} \hat{x}_{01} & \frac{a_1\hat{x}_{01} + 2\hat{x}_{02}}{2\omega} \\ \hat{x}_{02} & -\frac{2a_2\hat{x}_{01} + a_1\hat{x}_{02}}{2\omega} \end{bmatrix}, \tag{30}$$

$$A_2 = \begin{bmatrix} -\frac{a_1 v + z}{a_2} & \frac{v(4\omega^2 - a_1^2) - 2a_1 z}{4a_2\omega} \\ v & \frac{a_1 v + 2z}{2\omega} \end{bmatrix}, B_2 = \begin{bmatrix} \frac{a_1 v + z}{a_2} \\ -v \end{bmatrix}, \tag{31}$$

$$A_3 = \begin{bmatrix} -\frac{a_1 m + n}{a_2} & \frac{m(4\omega^2 - a_1^2) - 2a_1 n}{4a_2\omega} \\ m & \frac{a_1 m + 2n}{2\omega} \end{bmatrix}, B_3 = \begin{bmatrix} \frac{a_1 m + n}{a_2} \\ -m \end{bmatrix}. \tag{32}$$

With these definitions, (21) can be written as

$$A_1 \begin{bmatrix} X(t_s) \\ Y(t_s) \end{bmatrix} + A_2 \begin{bmatrix} X(t_s) \\ Y(t_s) \end{bmatrix} + B_2 = A_3 \begin{bmatrix} X(-\tau) \\ Y(-\tau) \end{bmatrix} + B_3. \tag{33}$$

Finally let

$$\begin{aligned} A_0 &= A_3^{-1}(A_1 + A_2), \\ B_0 &= A_3^{-1}(B_2 - B_3). \end{aligned} \tag{34}$$

Then (33) can be rewritten as

$$A_0 \begin{bmatrix} X(t_s) \\ Y(t_s) \end{bmatrix} + B_0 = \begin{bmatrix} X(-\tau) \\ Y(-\tau) \end{bmatrix}. \tag{35}$$

The switching and final time of the bang-bang control can be calculated by solving (35) for t_s and τ. This can be interpreted as finding the crossing point of the curves defined by the two sides of (35). Note that the left hand-side is an affine transformation of the curve on the right hand side. From (35), we see one curve is defined by increasing parameter and one from decreasing parameter. We therefore split the curve into two pieces: the *switching time* curve for $t > 0$ and the *final-time* curve for $t < 0$. This is illustrated graphically in Fig. 1, which shows an (X,Y) trajectory of a rest-to-rest switching between two set-points. In this figure, the crossing point is denoted M. The unit circle denotes the splitting of the spiral into the switching-time curve ED, located inside of the unit circle, and the final-time curve EM, located outside of the unit circle.

Note that the spiral curve is given by (29) and is thus determined only by the characteristic polynomial of the system. The affine mapping, however, is defined by (A_0, B_0) in (35) and depends not only on the system dynamics, but

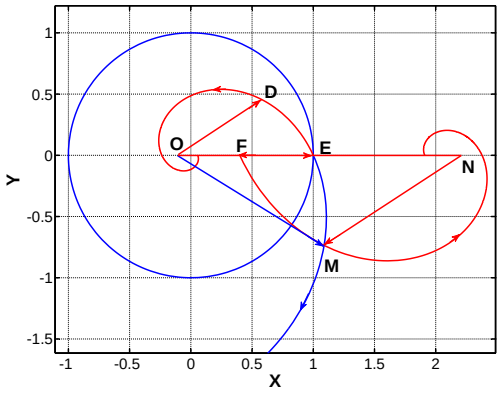

Fig. 1. A typical phase plane plot of a rest-to-rest bang-bang control. The spiral curve defined by (29) is separated by the unit circle into two segments. One segment is the switching-time curve ED inside the circle and the other is the final-time curve EM outside the circle. The switching-time curve is mapped to the curve FM by an affine mapping and crosses with the final-time curve EM at point M. The switching and final time can be calculated from the coordinates of the point M.

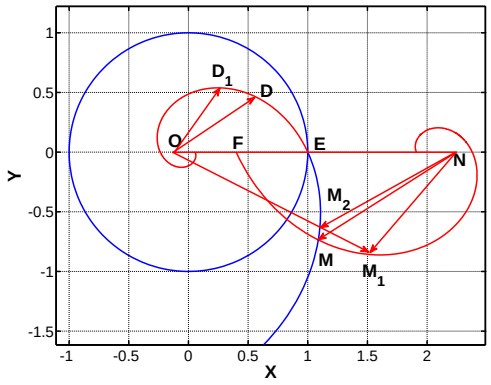

Fig. 2. Numerical calculation procedure of the coordinates of the point M. Given an initial guess $\angle EOD_1$, $\angle DOD_1$ can be estimated by calculating $\angle M_1NM_2$. Points M_1, M_2 will converge to point M and point D_1 will converge to point D quickly by adapting $\angle EOD_1$.

also on the initial state and input bounds of the system. FM is the image of the switching-time curve ED under the affine mapping. The parameter value $t = 0$, corresponds to the point $E = (1,0)$. As the parameter is increased, the vector $\overrightarrow{OE}$ rotates anticlockwise along ED and its image $\overrightarrow{NF}$ rotates anticlockwise along FM until it crosses the final-time curve EM at point M. Under the mapping, this point corresponds to the point D. By finding the coordinates of point D and point M, the switching time and final time of the bang-bang control can be calculated from (25) and (29).

Unfortunately, there is no analytic solution for the coordinates of the points D and M. However, as illustrated in Fig. 2, they can be solved efficiently using using the following numerical algorithm.

Step 0: Defining a stopping criterion $\varepsilon > 0$ and give an initial guess of $\angle EOD$ as $\angle EOD_1$.

Step 1: Calculate the coordinates of points D_1 and its image point M_1 under the affine mapping.

Step 2: Calculate the coordinates of points M_2 and $\angle M_1NM_2$.

Step 3: Let $\angle EOD_1 = \angle EOD_1 - \gamma\angle M_1NM_2$, where γ is a gain factor.

Step 4: Repeat step 1 to 3 until $\|M_1 - M_2\| < \varepsilon$.

IV. Simulation and Experimental Results

We ran both simulation and experiments to demonstrate the feasibility of our scheme. We applied the above method to calculate the bang-bang control to drive a single axis of a 3-D piezoelectric nanopositioning stage (Nano-PDQ, Mad City Labs) from one set point to another. The stage is equipped with a position sensor with accuracy on the order of picometers as reported by manufacturer. It was operated in closed-loop mode with a proportional-integral (PI) feedback controller provided by manufacturer. A data

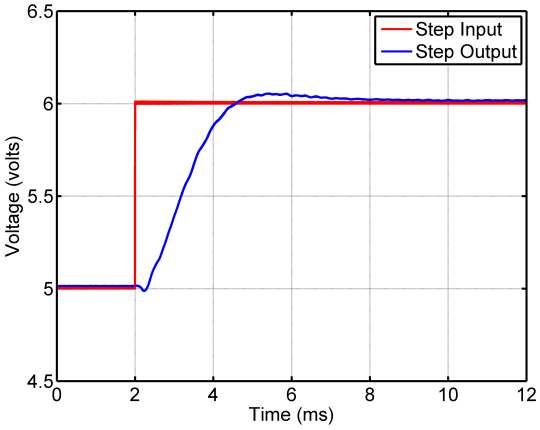

Fig. 3. Experimental step response of the nano-positioning stage. A 5 volts to 6 volts step signal was inputted to the nano-positioning stage controller. Both the step input signal and output signal from stage position sensor were sampled with a sampling frequency of 500 KHz.

acquisition card (NI-6259, National Instrument) was used to output the command signal to the stage controller and to sample stage position from its position sensor. Both the input and output signals of the data acquisition card range were limited to $[0,10]$ volts. The stage position was represented by the output voltage of the position sensor. We considered a simple step from the set point 5 volts to the set point 6 volts.

A. Bang-bang Control Design

The transfer function of the stage was estimated by driving the stage in close-loop mode with a step signal from 5 volts to 6 volts. The step signal and the stage response are shown in Fig. 3. The stage transfer function identified from the step response was

$$G(s) = \frac{-261.82s + 1.8143 \times 10^6}{s^2 + 1983.3s + 1.8118 \times 10^6}. \qquad (36)$$

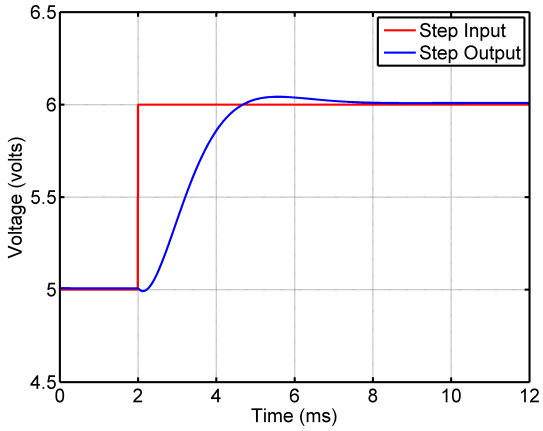

Fig. 4. Simulated step response of the nano-positioning stage for set point change from 5 volts to 6 volts based on the identified model from the experimental step response in Fig. 3.

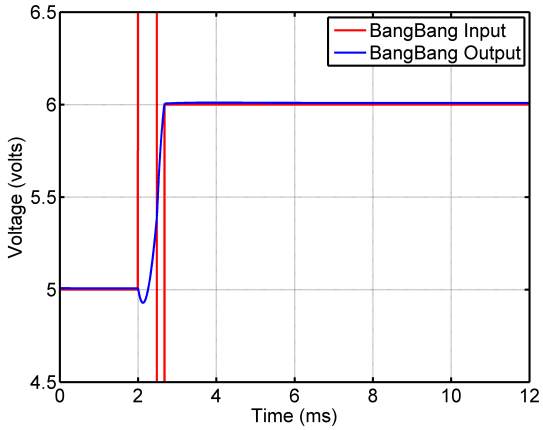

Fig. 5. Simulated bang-bang control response of the nano-positioning stage for set point change from 5 volts to 6 volts. The switching and final time were calculated as $t_s = 0.48075$ ms and $t_f = 0.67958$ ms. The control signal bound was set to $u \in [0, 10]$ volts.

Given the stage transfer function (36), the canonical controllable state-space model can be written as

$$A = \begin{bmatrix} 0 & 1 \\ -1.8118 \times 10^6 & -1983.3 \end{bmatrix}, \tag{37a}$$

$$B = \begin{bmatrix} -261.82 \\ 2.3336 \times 10^6 \end{bmatrix}. \tag{37b}$$

The initial and target state corresponding to the set points 5 and 6 volts respectively were calculated as

$$X_0 = \begin{bmatrix} 5.0072 \\ 1309.1 \end{bmatrix}, \quad X_r = \begin{bmatrix} 6.0086 \\ 1570.9 \end{bmatrix}. \tag{38}$$

With the control signal bounds $u_{min} = 0$ volts and $u_{max} = 10$ volts, the affine mapping defined by A_0 and B_0 was calculated from (30),(31),(32) and (34) as

$$A_0 = \begin{bmatrix} -0.8333 & 0 \\ 0 & -0.8333 \end{bmatrix}, \quad B_0 = \begin{bmatrix} 1.6667 \\ 0 \end{bmatrix}. \tag{39}$$

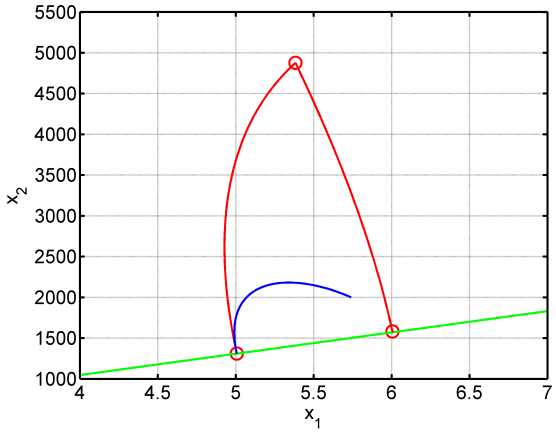

Fig. 6. Simulated state trajectories of system (3) under step and bang-bang control signal for $t \in [0, t_f]$. Both initial and target states locate on the steady-state line (green). Both state trajectories start from the initial state. The bang-bang trajectory (red) gets to the target state before the step trajectory (blue) does.

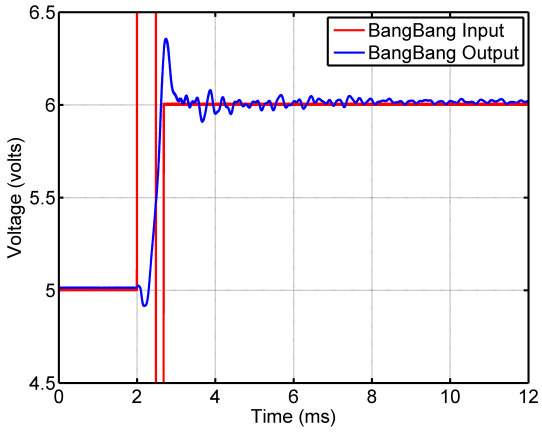

Fig. 7. Experimental bang-bang control response of the nano-positioning stage for set point change from 5 volts to 6 volts. The switching and final time were calculated as $t_s = 0.48075$ ms and $t_f = 0.67958$ ms. The control signal bound was $u \in [0, 10]$ volts. Both the bang-bang control signal and output signal from stage position sensor were sampled with sampling frequency 500 KHz.

The coordinates of point D and point M were calculated numerically as

$$D = \begin{bmatrix} 0.5623 \\ 0.2631 \end{bmatrix}, \quad M = \begin{bmatrix} 1.1981 \\ -0.2192 \end{bmatrix}. \tag{40}$$

From (25) and (29), we have

$$t_s = 0.48075 \text{ ms}, \quad t_f = 0.67958 \text{ ms}$$

B. Simulation Results

A simulation program was constructed in Matlab to simulate the response and state-space trajectory of the stage under the above step and bang-bang control signal. Fig. 4 shows the step response of the stage. Note that it matches very well

with the experimental result in Fig. 3. The simulated stage response under the bang-bang control signal is also shown in Fig. 5. The stage rests at the target position right at the end of the control, demonstrating the feasibility of our approach. The transition time for the set point change of the stage from 5 volts to 6 volts was reduced from approximatley 6 ms using the step control to 0.68 ms using the bang-bang control. The state trajectories under the step and the bang-bang control are shown in Fig. 6. The green line is the steady states corresponding to the set points of the stage. The blue curve is the state trajectory under the step input for $t \in [0, t_f]$. The red curve is the state trajectory under bang-bang control signal for $t \in [0, t_f]$. The two circle markers on the green line are the initial and target state respectively. The top circle marks the switching state of the bang-bang control.

C. Experimental Results

We also applied the designed bang-bang control signal to drive the real stage. The bang-bang control signal was output to the stage controller and the stage position sampled with a sampling frequency of $F_s = 500$ kHz by the data acquisition card. The result in Fig. 7 shows that the stage was driven to the target position at the end of the control. However, due to the modeling error and parameter uncertainty, the stage passed over the target position, rather than sitting there as in the simulation. Due to the closed loop controller, the stage did settle gradually to the target position after the residual vibration damped out. To suppress the unwanted overshoot and residual vibration caused by the unmodeled dynamics and parameter uncertainty, one can apply input shaping or other filtering techniques to smooth the input signal to get proximate time-optimal response with minimal excitation of unmodeled high-order modes [25], [10].

V. Conclusions

We have proposed a new approach to calculate the switching and final time of the bang-bang control for a stable second-order system. We have shown that the switching-time curve and the final-time curve are spirals determined by the natural frequency and damping ratio of the second-order system. An affine mapping, determined by the system dynamics, the initial state and the control signal bounds, determines the switching time and final time. This can be readily calculated by finding the cross point of the final-time curve with the image of the switching-time curve under the mapping. Both the simulation and experimental results demonstrated the feasibility of this approach. This approach tells us not only the switching time for the time-optimal control, but also how long the transition takes. This is particularly important when we want to optimize the visiting sequence to minimize the total visiting time over a collection of states before they are actually visited by the system. The extension of this approach to unstable and higher order system is an interesting and open question.

VI. Acknowledgements

This work was supported in part by the National Science Foundation through grant DBI-064983.

References

[1] S. B. Andersson and D. Y. Abramovitch, "A survey of non-raster scan methods with application to atomic force microscopy," pp. 3516–3521, 2007.

[2] S. B. Andersson, "Curve tracking for rapid imaging in afm," *IEEE Transactions on Nanobioscience*, vol. 6, no. 4, pp. 354–361, 2007.

[3] A. E. Bryson and Y.-C. Ho, *Applied Optimal Control: Optimization, Estimation, And Control*, 1975.

[4] J. Wing and C. A. Desoer, "The multiple-input minimal time regulator problem (general theory)," *IEEE Transactions on Automatic Control*, pp. 125–136, 1963.

[5] L. Y. Pao and G. F. Franklin, "Proximate time-optimal control of third-order servomechanisms," *IEEE Transactions on Automatic Control*, vol. 38, no. 4, pp. 560–580, 1993.

[6] W. S. Newman, "Robust near time-optimal control," *Automatic Control, IEEE Transactions on*, vol. 35, no. 7, pp. 841–844, 1990.

[7] M. L. Workman, R. L. Kosut, and G. F. Franklin, "Adaptive proximate time-optimal servomechanisms: Discrete-time case," in *Proceedings of the 26th Conference on Decision and Control*, Los Angeles, 1987, pp. 1548–1553.

[8] M. L. WORKMAN and G. F. FRANKLIN, "Implementation of adaptive proximate time-optimal controllers," pp. 1629–1635, 1988.

[9] F. F. Gene, L. W. Michael, and P. Dave, *Digital Control of Dynamic Systems*. Addison-Wesley Longman Publishing Co., Inc., 1997, 550726.

[10] C. La-orpacharapan and L. Y. Pao, "Shaped time-optimal feedback control for disk-drive systems with back-electromotive force," *IEEE Transactions on Magnetics*, vol. 40, no. 1, pp. 85–96, 2004.

[11] L. Y. Pao and C. La-orpacharapan, "Shaped time-optimal feedback controllers for flexible structures," *Journal of Dynamic Systems, Measurement, and Control*, vol. 126, no. 1, pp. 173–186, 2004.

[12] W. Singhose and L. Pao, "A comparison of input shaping and time-optimal flexible-body control," *Control Engineering Practice*, vol. 5, pp. 459–467, 1997.

[13] L. Y. Pao and W. E. Singhoses, "Robust minimum time control of flexible structures," *Automatica*, vol. 34, no. 2, pp. 229–236, 1998.

[14] B. K. Kim, W. K. Chung, H. S. Lee, H.-T. Choi, H. Suh, and Y. H. Chang, "Robust time optimal controller design for hard disk drives," *IEEE Transactions on Magnetics*, vol. 35, no. 5, pp. 3598–3600, 1999.

[15] S. Kim and D.-S. Choi, "Time-optimal control of state-constrained second- order systems and an application to robotic manipulators," pp. 1478–1483, 2002.

[16] A. Piazzia and A. Visioli, "Using stable input-output inversion for minimum-time feedforward constrained regulation of scalar systems," *Automatica*, vol. 41, pp. 305–313, 2005.

[17] D. Iamratanakul and S. Devasia, "Minimum-time/energy output-transitions in linear systems," pp. 4831–4836, 2004.

[18] W. S. Newman and K. Souccar, "Robust, near time-optimal control of nonlinear second-order systems: Theory and experiments," *Journal of Dynamic Systems, Measurement, and Control*, vol. 113, no. 3, pp. 363–370, 1991.

[19] K. H. You and E. B. Lee, "Robust, near time-optimal control of nonlinear second order systems with model uncertainty," in *Control Applications, 2000. Proceedings of the 2000 IEEE International Conference on*, 2000, pp. 232–236.

[20] B. Hredzak, G. Herrmann, and G. Guo, "A proximate-time-optimal-control design and its application to a hard disk drive dual-stage actuator system," *IEEE Transactions on Magnetics*, vol. 42, no. 6, pp. 1708–1715, 2006.

[21] T. Sun and S. B. Andersson, "Precise 3-d localization of fluorescent probes without numerical fitting," *Engineering in Medicine and Biology Society, 2007. EMBS 2007. 29th Annual International Conference of the IEEE*, pp. 4181–4184, 2007.

[22] S. Andersson and T. Sun, "Linear optimal control for tracking a single fluorescent particle in a confocal microscope," *Appl Phys B*, vol. 94, pp. 403–409, 2009.

[23] Z. Shen and S. B. Andersson, "LQG-based tracking of multiple fluorescent particles in two-dimensions in a confocal microscope," pp. 1682–1687, 2009.

[24] J. Wen and A. A. Desrochers, "A minimum time control algoritrm for linear and nonlinear systems," pp. 1441–1446, 1985.

[25] H. T. Ho, "Fast servo bang-bang seek control," *IEEE Transactions on Magnetics*, vol. 33, no. 6, pp. 4522–4527, 1997.